Study of Environmental Survivability and Stability of Folded MEMS IMU

Yu-Wei Lin, Alexandra Efimovskaya, and Andrei M. Shkel
MicroSystems Laboratory
University of California, Irvine, CA, USA
Email: {yuweil4, aefimovs, andrei.shkel}@uci.edu

***Abstract*—This paper presents a study on the structural rigidity of an Inertial Measurement Unit (IMU) implemented using the Folded MEMS approach. For such folded structures, environmental survivability and stability is a natural concern. We investigated IMUs of 35 mm^3 (small) and 130 mm^3 (medium) in volume, in the shape of a cube and a pyramid, and considered the reinforcement methods, including epoxy, eutectic solder, and silicon welding. Experimental characterization of a medium cube with eutectic reinforcement showed the maximum tilt of 0.2 mrad on the cube's sidewalls under temperature variation 25°C-90°C and the tilt of 0.2mrad under 10Hz to 20kHz vibration. An IMU error model was implemented, with the target sensors performance of tactical-grade, using in-run bias stability and scale factor (SF) stability for gyroscope (1°/hr, 100ppm) and for accelerometer (100μg, 100ppm), and a pre-defined trajectory with 122s flight time. The 0.2 mrad misalignment for the medium eutectic-soldered cube corresponded to a Circular Error Probable (CEP) rate of 1.25 nmi/hr, and a typical tactical grade IMU corresponded to CEP rate $\leq$1nmi/hr. We also concluded that the 35mm^3 eutectic-bonding reinforced cubes will survive the mechanical shock under 10,000g, while silicon welding reinforced cubes of 35 mm^3 would survive the shocks of 20,000g.**

***Keywords*—3D-MEMS, Inertial Measurement Unit, IMU, Vibration, Mechanical Shock, Temperature, Parylene**

I. Introduction

Miniaturization of high performance MEMS Inertial Measurement Unit (IMU) not only improves compatiblity with military applications through reduction in size, weight and power (SWaP), but also enables a wider range of applications in consumer electronics, automotive, biomedical, and robotics industries. The main methods to fabricate MEMS chip-scale high-performance IMU can be categorized into two approaches: a single-chip with multiple single-axis or multi-axis sensor(s), [1], or a PCB module assembly of single-axis sensors, [2]. Recently, several research groups have made advances in the hybrid approach, such as the multi-layer stacked IMU, [3], and the tri-fold integrated IMU, [4]. Our solution to miniaturization of tactical-grade IMU is through the folded IMU approach, [5], which combines the advantage of high performance single-axis sensors, and the ability to have 6-DOF sensitivity in a miniaturized footprint IMU. This is accomplished by fabricating foldable MEMS structures on a wafer-level and assembling them into 3D cubic or pyramidal configurations. The sensitive axis of each sensor is dependent on design geometries and also requires an assembly process to maintain the precision of alignment.

Many applications require high performance IMU and they also require the IMU to undergo intense vibration (5Hz-20kHz, 20g amplitude), shock (up to 20,000g), and temperature variations (-54°C to 85°C), [6]. These environmental factors can greatly affect the accuracy and stability of the IMU. Environmental performance of the folded MEMS IMU can be separated into two focused areas: (1) the performance of sensors' elements under variations in vibration, shock, and temperature; (2) and the stability of the platform (folded substrates) that carries the sensors. In this paper, we focus only on the survivability and stability of the folded MEMS backbone structure. An initial structural rigidity study under variations in temperature, vibration, and shock for a folded pyramid was conducted in [5]. We expanded the scope of our previous study beyond consideration of reinforcement materials, and investigated the effect of size and geometry in environmental tests. Not only did we demonstrate the precision of alignment that sensors can maintain after fabrication and assembly, we also estimated the effect of these misalignment errors through a simple error model.

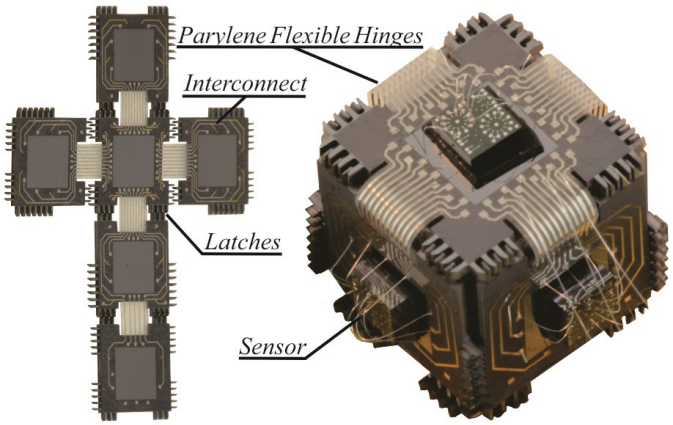

Fig. 1. Fabricated folded IMU structure before (left) and after (right) folding

II. Folded IMU Backbone-Structure Fabrication

Prototype of 3D MEMS origami-like IMU has previously been demonstrated in [5]. The updated double-sided process has been shown in [7] with in-situ fabricated sensors, and integration with separately fabricated sensors, [8]. Fig.2 shows the fabrication flow for the folded IMU backbone structure using silicon wafer, and in the blue box, the figure shows the case where sensors are co-fabricated using a SOI wafer.

The fabrication process, [8], starts with deposition and patterning of 50 nm thick chromium adhesion layer. Parylene is then deposited using the SCS PDS 2010 tool from Specialty Coating System using the standard parameters, [9]. The thickness of the parylene layer for samples ranges from 12 to 18 μm, depending on sample location inside the deposition

This material is based upon work supported by the DARPA grant N66001-13-1-4021.

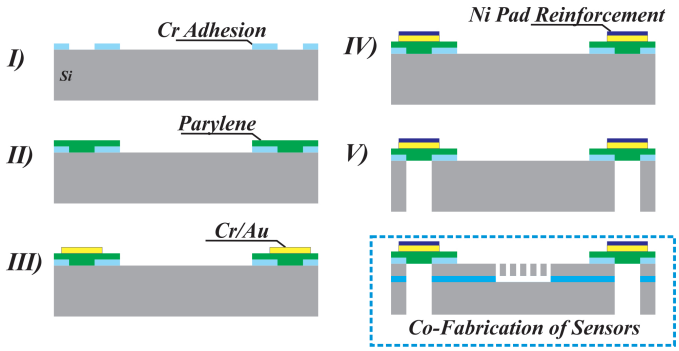

Fig. 2. Fabrication flow of IMU back-bone structure

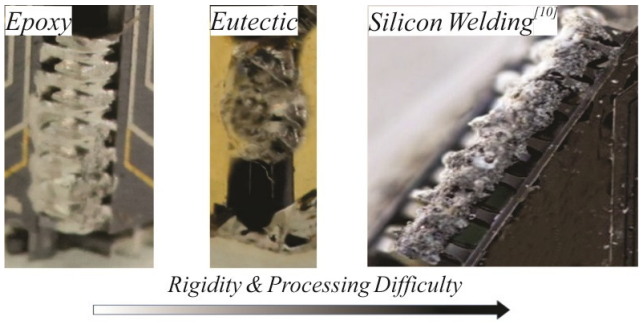

Fig. 3. Latch reinforcement materials

chamber. Etching of parylene is performed by patterning a 150 nm thick titanium mask and oxygen plasma. The Ti mask can be removed either by plasma etching with CF_4 gas or wet etching with diluted hydrofluoric acid. 50 nm of chromium and 500 nm of gold are evaporated and patterned as metal traces. On top of the Cr/Au metal traces, nickel (0.5-1 μm) is electroplated to allow for wirebonding. Wirebonding without the nickel reinforcement will result in penetration of the gold layer and a "scratch" on the underlying parylene layer. The IMU sidewall panels are DRIE etched and the foldable structure is released from the rest of the wafer, as shown as a flat structure in Fig.1.

Currently, the flat structure is folded manually by aligning the interlocking latches; however, the process is scalable. The interlocking latches are then reinforced with the proposed methods: 8331 silver conductive epoxy, 80Au20Sn solder, and silicon welding (Fig.3). The order of methods corresponds to increasing difficulty in preparation, and to increasing mechanical strength and stability. The silver epoxy can readily be applied to the folded structure. The samples for the eutectic solder method require an additional step of Cr/Au coating on the back-side of the IMU structure in order for the solder to wet the bonding surfaces. Silicon welding will require a powerful laser and focusing optics. Feasibility of silicon welding for thick silicon structure and integration with the folded IMU process has been demonstrated in [10]; however, it has not been experimentally performed in this paper and our results for silicon welded sample are simulated.

III. Experimental Setup

A. Structural Misalignment due to Temperature and Vibration

An optical characterization method was adapted from [4] and [5] to measure the relative change in angle of the folded

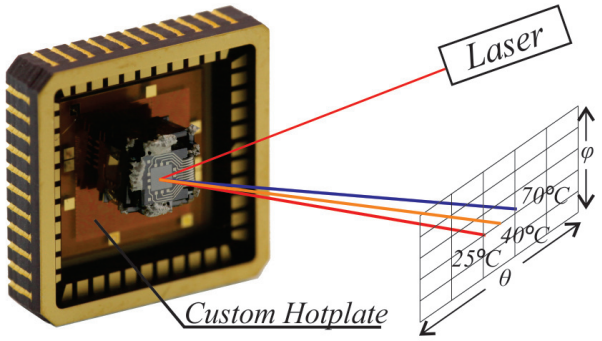

Fig. 4. Temperature misalignment experimental setup

structure's sidewalls. The measurement was achieved by pointing a collimated laser beam on the surface of the folded structure, during which the system is calibrated. The change in relative displacement of the laser beam's reflection was recorded on a detection screen, Fig. 4.

The setup was prepared on an optical table, where the position of the LCC package socket was fixed. For calibration, the laser point on the surface of the folded structure was picked as reference. The distances and angles from the reference point to the laser (0.15m, θ_1, ϕ_1) and to the detection screen (1.5m, θ_2, ϕ_2) were measured. In the case of temperature experiment, a custom hotplate was made from borosilicate glass and Cr/Au metal traces. The die was mounted onto the custom made hotplate using eutectic alloy. The temperature was voltage controlled and monitored by an IR camera (FLIR a655sc). The measured displacement is the aggregate displacement of all the sidewalls and includes the stress and displacement induced by the die attachment (eutectic bonded for all samples) to the folded structure. The experiment on structural misalignment due to vibration was performed similarly to the temperature experiment, with measurements taken before and after the vibration excitation.

B. Vibration

The vibration experiment was conducted using a SPEKTRA SE-09 vertical shaker and a Polytec OFV-534 Laser Doppler Vibrometer (LDV). The folded IMU structures were excited by sinusoidal vibrations at 20Hz to 50,000Hz, and the responses were measured by the LDV throughout the frequency sweep (top left of Fig. 6). Vibration data was collected both at the top of the sidewalls and also at the base mount of the cubic structure. The difference between the two data-sets eliminated the vibration modes caused by the mounting setup.

C. Mechanical Shock

The mechanical shock was simulated in COMSOL Multiphysics. The base of the structure (cube/pyramid) was fixed using a circular shaped boundary constraint that simulated the eutectic die-attachment interface. The sidewalls of the structure had 50 μm separation and were rigidly connected by the reinforcement material, which was defined as cylinders running along the interlocking latches. A body load described by a half-sine peak to peak value of 20,000g acceleration with 5 ms duration was applied in all x-y-z directions. The time dependent modeling studies were performed for folded structures of different sizes, shapes, and reinforcement materials.

TABLE I. ANGULAR MISALIGNMENT OF FOLDED IMU STRUCTURE REINFORCED BY DIFFERENT METHOD

	Epoxy		Eutectic	
	Med (mrad)	Sm (mrad)	Med (mrad)	Sm (mrad)
Temperature (25°C to 90°C)	4.1	6.6	0.2	0.4
Cooled to RT after heating	1.1	2.9	0.2	0.3
Vibration (10Hz to 20kHz)	0.8	1.2	0.2	0.2

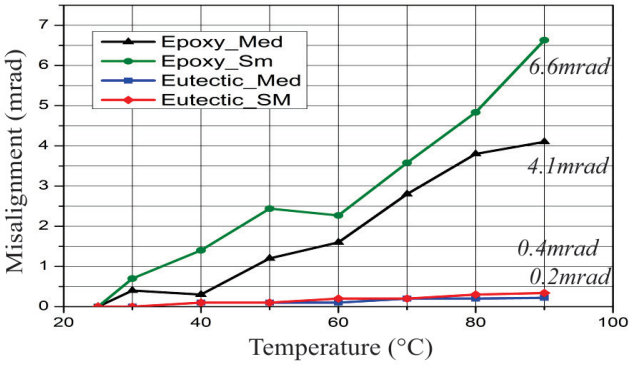

Fig. 5. Sidewall misalignment from temperature variation for IMU of different sizes and reinforcements

IV. RESULTS AND DISCUSSION

A. Structural Misalignment due to Temperature and Vibration

The results of the sidewall misalignment study are summarized in Table I. The first row of the table corresponds to 90°C data in Fig.5, which presents the result from 25°C to 90°C temperature variation. The second row of the table shows the misalignment of each sample after cooling back to room temperature. The maximum displacement of 6.6 mrad was observed on a small epoxy-reinforced cubes, and a minimum displacement of 0.2 mrad on the medium eutectic-reinforced cubes. Given by the same expansion displacement of the reinforcement material, the displacement will translate to a larger angle for a smaller structure. The general military temperature range is between -54°C and 85°C, and in this paper, we explored temperatures above room temperature (+25°C) and assumed a linear coefficient of thermal expansion and contraction for the full military temperature range. In terms of repeatability, results from a similar experiment in [4] showed that even if the initial sidewall misalignment was different, the relative change in alignment is comparable for a single sample going through several thermal cycle and for different samples of the same reinforcement method.

B. Vibration

Apart from the vibration experiment, finite element models were developed for all cubes with a combination of sizes and reinforcement methods. Table II shows the first two modes of each cube, both from finite element analysis and experimental study. Fig.6 shows no peak before 11kHz for the small eutectic-soldered cube, and excitation mode for the epoxy reinforced medium cube occurred as early as 6.5kHz. The lower frequency in the experimental result compared to finite element analysis might be explained by imperfections in the bonding interface. The process tuning will be needed for both methods (epoxy and eutectic solder) to fully fill the gaps between the interlocking latches and create a void-free bond.

TABLE II. EIGEN-FREQUENCY OF REINFORCED CUBIC STRUCTURES

	First two eigen-frequencies			
	Sm (FEA)	Sm (Exp.)	Md (FEA)	Md (Exp.)
Epoxy	13kHz 28kHz	12kHz 14.6kHz	8.3kHz 18kHz	6.2kHz 8.1kHz
Au/Sn Solder	17kHz 44kHz	11.5kHz	8.6kHz 25kHz	9.1kHz

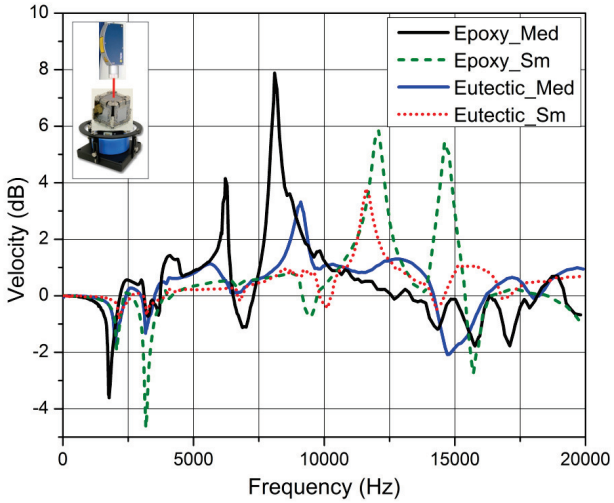

Fig. 6. Vibration from 10Hz-160Hz with 1g to 20g amplitude(log ramping), and 160Hz-20kHz constant 20g amplitude

C. Mechanical Shock

Table III shows the time dependent modeling studies' result from COMSOL Multiphysics. The silicon-welded small cube and silicon-welded pyramid had the least stress of 377 MPa and 486 MPa, respectively. Assuming the welded silicon latches have poly-crystalline structure, the structure will not fail under gun-hard conditions compared to the 3000 MPa yield strength of polycrystalline silicon and 7000 MPa of single-crystalline silicon for the rest of the structure.

Table IV summarizes the trade-off between structural size, geometry, and reinforcement methods. Smaller size provided a better vibration and shock rigidity and stability, but had higher sidewall misalignment due to temperature. Cube and pyramid were comparable in temperature and vibration experiments, but pyramid was a lot more shock resistant. Finally, the silicon welding will be necessary for structures to survive the high shock and should be used to improve structural stability in terms of vibration and temperature misalignment.

D. CEP Model

An intuitive measurement of the accuracy of a guidance system is to be defined by the Circular Error Probable (CEP). We use this metrics to represent the errors generated by instability of the folded IMU and their implication. When the CEP value is defined by n meters, there is a 50% chance of landing within n meters of the target destination, while CEP rate, in nmi/hr, gives an indication on how fast the error is accumulating.

TABLE III. FINITE ELEMENT OF SHOCK ON FOLDED IMU STRUCTURE REINFORCED BY EPOXY, EUTECTIC, AND WELDING

	Maximum Stress (Occurs near bonding interface)			
	Cube 130mm^3	Cube 35mm^3	Pyramid 145mm^3	Material Yield Strength
Silver Epoxy	3220 MPa	971 MPa	1660 MPa	6.28 MPa
Au/Sn Solder	1750 MPa	851 MPa	1260 MPa	275 MPa
Silicon Welding	1050 MPa	377 MPa	486 MPa	3000 MPa*

*yield strength of poly-crystalline silicon

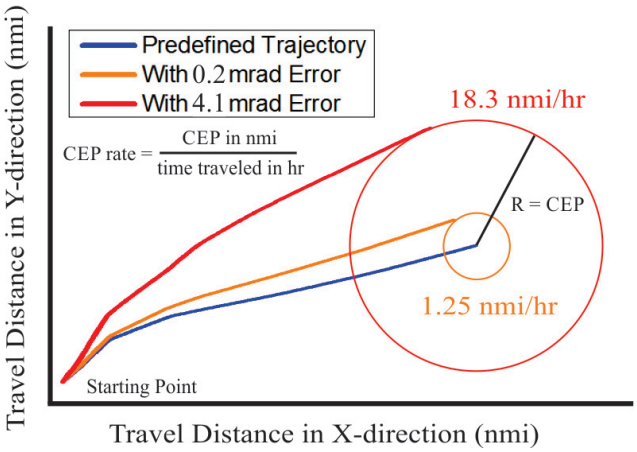

Fig. 7. Representation of Trajectories from IMU Error Model for CEP Calculation

A simple error model was adapted from [10]. The model accounted for error accumulations caused by in-run bias stability and scale-factor (SF) stability of a tactical grade gyroscope (1°/hr, 100ppm) and an accelerometer (100μg, 100ppm), as well as the change in orientation of the sensor axes of sensitivity (Table I). A path generation code was implemented to generate a pre-defined trajectory that mimics a short range ballistic missile with maximum velocity of 2413 m/s, maximum acceleration of 1264 m/s^2, and travel time of 122 seconds. After navigating the pre-defined trajetory, the eutectic-soldered medium cube had CEP rate of 1.25 nmi/hr (Fig. 7), indicating the IMU can preserve the tactical grade performance on the order of 15 seconds. The reinforcement by silicon welding should improve the performance closer to the no-misalignment-case of 0.38 nmi/hr.

V. CONCLUSION

MEMS IMU backbone structures had been batch fabricated using the folded MEMS approach. Structures of different sizes (35mm^3/130mm^3) and geometry (cube/pyramid) were folded and reinforced with methods including epoxy, eutectic solder, and silicon welding. Laser system has been used to measure the sidewall misalignment of the folded structure caused by temperature variation and vibration. The 4.1 mrad and 0.2 mrad sidewall misalignment corresponded to the medium cube reinforced by epoxy and the medium eutectic-soldered cube, respectively, which translated to 18.3 nmi/hr and 1.25 nmi/hr Circular Error Probable (CEP) rate. Vibration (experimental) and shock (finite-element) analysis were also conducted for structural survivability assessment. Trade-offs between structural size, geometry, and reinforcement methods were established, with smaller structure being more vibration and shock resistant, and less favorable for precise sensor axis alignment; pyramids were more shock resistant than cubes; and although the most difficult to fabricate, silicon welding will be required for structures to survive 20,000g shock.

TABLE IV. TRADE-OFF BETWEEN SIZE, GEOMETRY, AND REINFORCEMENT MATERIALS VS. ENVIRONMENTAL CONDITIONS

		Temperature	Vibration	Shock
Size	Small (35mm^3)			
	Med (130mm^3)			
Geometry	Cube (130mm^3)			
	Pyramid (145mm^3)	[5]	[5]	
Material	Epoxy			
	Eutectic			
	Welding			

Survives the condition and performs better than other option(s)
May not survive the condition or out-performed by other option(s)
Theoretically better than eutectic solder, but need to be verified

ACKNOWLEDGMENT

Devices were designed and tested at the MicroSystems Laboratory, UC Irvine. Fabrication of the devices was performed at the Integrated Nanosystems Research Facility (INRF) at UC Irvine.

REFERENCES

[1] A. Devices. (2016) ADIS16460. [Online]. Available: http://www.analog.com

[2] Honeywell. (2012) HG1930 IMU. [Online]. Available: http://www.honeywell.com

[3] Z. Cao, Y. Yuan, G. He, R. Peterson, and K. Najafi, "Fabrication of multi-layer vertically stacked fused silica microsystems," in *IEEE Transducers 2013 & Eurosensors XXVII*, Barcelona, Spain, June 16-20, 2013.

[4] W. Zhu, Y. Zhang, and N. Yazdi, "A Batch-Mode Assembly and Packaging Technology for 3-Axis Tri-Fold Inertial Measurement Units," in *IEEE ISISS 2014*, Laguna Beach, CA, USA, February 24-25, 2014.

[5] S. A. Zotov, M. C. Rivers, A. A. Trusov, and A. M. Shkel, "Folded MEMS Pyramid Inertial Measurement Unit," *IEEE Sensors Journal*, vol. 11, no. 11, pp. 2780–2789, 2011.

[6] S. Habibi, S. J. Cooper, J.-M. Stauffer, and B. Dutoit, "Gun Hard Inertial Measurement Unit Based on MEMS Capacitive Accelerometer and Rate Sensor," in *IEEE/ION Position, Location and Navigation Symposium 2008*, Monterey, CA, USA, May 05-08, 2008.

[7] A. Efimovskaya, D. Senkal, S. Askari, and A. M. Shkel, "Origami-like Folded MEMS for Realization of TIMU: Fabrication Technology and Initial Demonstration," in *IEEE ISISS 2015*, Hapuna Beach, HI, USA, March 23-26, 2015.

[8] A. Efimovskaya, Y.-W. Lin, Y. Yang, E. Ng, Y. Chen, I. Flader, C. H. Ahn, V. Hong, T. W. Kenny, and A. M. Shkel, "On Cross-Talk Between Gyroscopes Integrated on a Folded MEMS IMU Cube," in *IEEE MEMS 2017*, Las Vegas, NV, USA, January 22-26, 2017.

[9] R. Robbins, "SCS Parylene Deposition Tool Manual," 2014. [Online]. Available: https://www.utdallas.edu/rar011300/Parylene/ParyleneDepManual.pdf

[10] M. C. Rivers, "Folded MEMS 3-D Structures for Inertial Measurement Applications," Ph.D. dissertation, University of California, Irvine, 2015.